Forest Ecology and Management 339 (2015) 71–86

Contents lists available at ScienceDirect

Forest Ecology and Management

journal homepage: www.elsevier.com/locate/foreco

Spatiotemporal dynamics of recent mountain pine beetle and western spruce budworm outbreaks across the Pacific Northwest Region, USA

Garrett W. Meigs[a,*], Robert E. Kennedy[b], Andrew N. Gray[c], Matthew J. Gregory[a]

[a] Department of Forest Ecosystems and Society, Oregon State University, 321 Richardson Hall, Corvallis, OR 97331, USA
[b] Department of Earth and Environment, Boston University, 675 Commonwealth Avenue, Boston, MA 02215, USA
[c] Pacific Northwest Research Station, USDA Forest Service, 3200 SW Jefferson Way, Corvallis, OR 97331, USA

ARTICLE INFO

Article history:
Received 11 August 2014
Received in revised form 21 November 2014
Accepted 30 November 2014

Keywords:
Bark beetle
Change detection
Defoliator
Forest disturbance
Landsat time series
Tree mortality

ABSTRACT

Across the western US, the two most prevalent native forest insect pests are mountain pine beetle (MPB; *Dendroctonus ponderosae*; a bark beetle) and western spruce budworm (WSB; *Choristoneura freemani*; a defoliator). MPB outbreaks have received more forest management attention than WSB outbreaks, but studies to date have not compared their cumulative mortality impacts in an integrated, regional framework. The objectives of this study are to: (1) map tree mortality associated with MPB and WSB outbreaks by integrating forest health aerial detection surveys (ADS; 1970–2012), Landsat time series (1984–2012), and multi-date forest inventory data; (2) compare the timing, extent, and cumulative impacts of recent MPB and WSB outbreaks across forested ecoregions of the US Pacific Northwest Region (PNW; Oregon and Washington). Our Landsat-based insect atlas facilitates comparisons across space, time, and insect agents that have not been possible to date, complementing existing ADS maps in three important ways. The new maps (1) capture variation of insect impacts within ADS polygons at a finer spatial resolution (30 m), substantially reducing estimated insect extent; (2) provide consistent estimates of change for multiple agents, particularly long-duration changes; (3) quantify change in terms of field-measured tree mortality (dead basal area). Despite high variation across the study region, spatiotemporal patterns are evident in both the aerial survey- and Landsat-based maps of insect activity. MPB outbreaks occurred in two phases – first during the 1970s and 1980s in eastern and central Oregon and then more synchronously during the 2000s throughout dry interior conifer forests of the PNW. Reflecting differences in habitat susceptibility and epidemiology, WSB outbreaks exhibited early activity in northern Washington and an apparent spread from the eastern to central PNW during the 1980s, returning to northern Washington during the 1990s and 2000s. At ecoregional and regional scales, WSB outbreaks have exceeded MPB outbreaks in extent as well as total tree mortality, suggesting that ongoing studies should account for both bark beetles and defoliators. Given projected increases of insect and fire activity in western forests, the accurate assessment and monitoring of these disturbances will be crucial for sustainable ecosystem management.

1. Introduction

Insects are important forest disturbance agents, influencing ecosystem structure, function, and dynamics from local to global scales. Across western North America, native forest insects affect more area annually than wildfire (e.g., Williams and Birdsey, 2003; Littell et al., 2009; Hicke et al., 2013), and, like wildfire, insects have received increasing research and public attention. In addition to their direct effects on forest mortality and succession, insects also influence fuel structure, setting the stage for potential interactions with fire, anthropogenic climate change, and forest management (e.g., McKenzie et al., 2004; Littell et al., 2010; Simard et al., 2011). Different insects vary substantially in their distribution and effects, however, and it is important to contrast the tree mortality impacts of different insect types.

In western North America, the two most prevalent native insects classified as forest pests are mountain pine beetle (MPB; *Dendroctonus ponderosae* Hopkins [Coleoptera: Scolytidae]; a bark beetle) and western spruce budworm (WSB; *Choristoneura freemani* Razowski [Lepidoptera: Tortricidae]; a defoliator) (Williams and Birdsey, 2003). Both insects exhibit cyclic outbreaks associated with endogenous and exogenous factors, including insect population dynamics, host tree vigor and distribution, and climatic

---

* Corresponding author. Tel.: +1 802 656 4279; fax: +1 802 656 8683.
E-mail address: gmeigs@gmail.com (G.W. Meigs).

http://dx.doi.org/10.1016/j.foreco.2014.11.030

variability (Sanders et al., 1985; Swetnam and Betancourt, 1998; Raffa et al., 2008; Bentz et al., 2010). Under sustained outbreak conditions, both insects can cause pervasive tree mortality and associated changes in forest structure and composition, although the mechanisms and rates differ (Swetnam and Lynch, 1993; Raffa et al., 2008; Meigs et al., 2011). MPB adults mass attack the stems of pine trees (*Pinus spp*., particularly mature lodgepole pine [*P. contorta* Douglas ex Louden]) to feed on cambium and lay eggs (Goheen and Willhite, 2006; Raffa et al., 2008), inducing variable but relatively rapid tree mortality across large areas (e.g., regional-scale outbreaks in British Columbia and US Rocky Mountains [Meddens et al., 2012]). In contrast, WSB larvae typically consume the current year's foliage of host trees (especially understory true firs [*Abies spp*.], spruces [*Picea spp*.], and Douglas-fir [*Pseudotsuga menziesii* (Mirb.) Franco]) (Sanders et al., 1985; Goheen and Willhite, 2006; Meigs et al., 2011). Despite these subtler impacts, multiple years of WSB defoliation can result in tree mortality, often in conjunction with secondary bark beetles (Hummel and Agee, 2003; Goheen and Willhite, 2006; Vogelmann et al., 2009). In the US Pacific Northwest Region (PNW; defined here as the states of Oregon and Washington), multiple widespread outbreaks of both insects have occurred in recent decades (Williams and Birdsey, 2003), creating a strong need for a multi-decadal, retrospective analysis of their impacts.

Although numerous studies have assessed the causes and consequences of MPB and WSB from fine to coarse scales (e.g., Swetnam and Lynch, 1993; Simard et al., 2011; Preisler et al., 2012; Meddens et al., 2012), few to date have compared their cumulative impacts at a regional scale (i.e., multiple ecological units, such as ecoregions, or political units, such as states; but see Williams and Birdsey, 2003). This lack of comparison is due in part to defoliators having more gradual effects than bark beetles (e.g., Vogelmann et al., 2009; Meigs et al., 2011); it is also due to a lack of spatiotemporally explicit datasets that quantify the impacts of various agents in consistent units. In this study, we present a novel mapping framework to compare bark beetle and defoliator effects on tree mortality in consistent units, integrating spatially and temporally extensive aerial, satellite, and field data across the PNW.

Here, we suggest that a broad, regional scale (such as the PNW) is essential to elucidate potentially unprecedented changes and emergent patterns. Particularly in the context of global change, it is important to evaluate recent insect outbreaks across spatiotemporal scales that are broad enough to capture multiple outbreaks of the same insect species (e.g., Swetnam and Betancourt, 1998; Meddens et al., 2012; Flower et al., 2014). In addition, a regional framework enables the comparison of multiple insect species, forest types, and emergent impacts not apparent at finer spatiotemporal scales. Moreover, a regional framework may allow researchers and managers to assess whether particular outbreaks are driven by landscape-scale endogenous drivers (e.g., host abundance and distribution, insect population dynamics) or regional-scale exogenous drivers (e.g., climate, synchronous drought stress of host trees). There are very few datasets spanning broad spatial and temporal scales, however, and existing maps have key limitations and uncertainties (Meigs et al., 2011; Meddens and Hicke, 2014). New, regionally extensive but fine-grained maps are necessary to advance our understanding of these insect outbreak phenomena and to provide an ecological basis for emerging restoration frameworks (e.g., Haugo et al., 2015).

In the western US, the most readily available maps to assess landscape and regional insect dynamics are forest health aerial detection surveys (ADS). These surveys provide an unmatched record of insect activity and other forest disturbances and have been collected annually for decades (Williams and Birdsey, 2003). Although valuable for coarse-scale assessments, ADS data have critical uncertainties related to the spatiotemporal variability of methodology, personnel, and observation conditions (Meigs et al., 2011; Preisler et al., 2012; Meddens and Hicke, 2014). More importantly, aerial surveys delineate insect effects within inclusive polygons that contain live trees, creating the appearance of widespread, homogeneous insect activity across entire landscapes and regions, whereas actual insect impacts on tree mortality are highly variable at finer scales (Meigs et al., 2011). In contrast to this potential overestimation of insect *extent* at the regional scale, studies have shown that the ADS units of damage, at least in the case of bark beetles, are a strong underestimate of actual *impacts* at the forest stand scale (Meigs et al., 2011; Meddens and Hicke, 2014). In addition, the ADS emphasis on detecting insect activity in a given year limits the potential to quantify lasting vegetation changes that manifest over multiple years. Finally, aerial surveys characterize different insects in different units (e.g., dead trees per unit area for bark beetles; relative defoliation units for defoliation), hindering their comparison. Thus, complementary geospatial and field datasets are necessary to facilitate regional analysis and address forest management concerns.

In many ways, the Landsat satellite archive represents an ideal complementary dataset. As reviewed by Wulder et al. (2006), Meigs et al. (2011), recent studies have used a variety of remote sensing platforms to map insect disturbance, and Landsat-based approaches show considerable promise for capturing durable vegetation decline and recovery. Due to its moderate spatial resolution (30-m grain), broad temporal scope (1984-present), and consistent, seamless coverage, the Landsat TM sensor captures a variety of disturbance dynamics at forest stand, landscape, and regional scales (Cohen and Goward, 2004; Kennedy et al., 2014). Previous studies have demonstrated wide variability in Landsat spectral responses associated with insect outbreaks (e.g., Vogelmann et al., 2009; Goodwin et al., 2010; Meigs et al., 2011; Meddens et al., 2013). Although more studies have focused on MPB outbreaks (due to their generally more damaging effects; e.g., Wulder et al., 2006; Goodwin et al., 2010; Simard et al., 2011), Landsat imagery has been used to track WSB dynamics as well (Vogelmann et al., 2009; Meigs et al., 2011). Like the ADS data, however, Landsat-based estimates have important limitations. Specifically, satellite data lack any inherent attribution of specific disturbance agents, and the raw reflectance data have limited biological meaning without being linked to ground-based estimates of change (e.g., tree mortality).

Here, we build on a recent pilot study (Meigs et al., 2011), applying new approaches across a much broader area to develop a regional, Landsat-based atlas of insect activity. Our overall goal is to map and compare the effects of two native insects on tree mortality across the PNW Region from 1970 to 2012. Our specific objectives are to: (1) map tree mortality associated with MPB and WSB outbreaks by integrating aerial detection surveys, Landsat time series, and multi-date forest inventory data; (2) compare the timing, extent, and cumulative impacts of recent MPB and WSB outbreaks across the forested ecoregions of Oregon and Washington.

2. Methods

2.1. Study area

The US Pacific Northwest is a geographically diverse region with ecologically, economically, and socially important forest landscapes. Mixed-conifer forests are widespread, and their composition and structure vary across gradients of climate, topography, soil parent material, and disturbance and management history (Franklin and Dyrness, 1973; Hessburg et al., 2000). Although precipitation and temperature regimes vary substantially, a common climatic feature is that little precipitation occurs in summer months (Franklin and Dyrness, 1973). The resulting warm, dry conditions, coupled with abundant biomass and slow decomposition, are conducive to periodic insect and wildfire disturbances (e.g., Littell et al., 2010). This study focuses on the forested ecoregions (Omernik, 1987) where MPB and WSB have been most active historically, which are primarily the drier interior mixed-conifer forests east of the crest of the Cascade Range (Fig. 1). According to aerial surveys, these two insects have influenced about one-third of the total forested ecoregion area since 1970 (ca. 8 M ha out of ca. 25 M ha; Fig. 1).

In general, US PNW forests inhabit remote, mountainous terrain and are managed primarily by the US Forest Service. These forest landscapes have undergone dramatic historical and recent anthropogenic changes, including widespread fire suppression and exclusion, logging, and grazing, which have increased the potential for landscape-to-regional-scale outbreaks of native bark beetles and defoliators (Hessburg et al., 2000). Given the widespread extent of similar geographic conditions and anthropogenic pressures, these forests and recent MPB and WSB dynamics are also broadly representative of analogous vegetation types and recent insect outbreaks throughout western North America.

2.2. Datasets

Here, we leverage three spatially and temporally extensive datasets in a retrospective, empirical framework to create new maps of MPB and WSB impacts (Fig. 2). In essence, we use aerial surveys to identify locations with known insect activity, Landsat time series to capture fine-grained spectral change in those locations, and multi-date forest inventory data to translate spectral change to field-based estimates of tree mortality.

2.2.1. Aerial detection survey (ADS)

The ADS is a cooperative effort between federal and state agencies, conducted nationally and administered at the regional level. In US Forest Service Region 6 (Oregon and Washington; data available online: http://www.fs.usda.gov/main/r6/forest-grassland-health/), these surveys have been conducted by observers in fixed-wing aircraft since 1947 with the objective of recording a wide range of forest insects and diseases based on characteristic aerial signatures (Ciesla, 2006). Compared to other regions in the western US (e.g., Rocky Mountains; Meddens et al., 2012), the PNW has been mapped by ADS more consistently and completely on an annual basis.

In this study, we utilized ADS data from 1970 to 2012, converted the polygons to raster format (30-m grain), and selected all MPB and WSB pixels for further analysis (Fig. 2). For each affected pixel, we identified the onset (first year of detection), cumulative magnitude (trees per hectare for MPB, defoliation units on an annual 1–3 scale for WSB), and count of years detected (as in Meigs et al., 2011) for two time periods (1970–2012, 1984–2012). Due to the uncertainties mentioned above, ADS data are not intended for assessment of specific stands or points on the ground but rather landscape-to-regional patterns and trends (Ciesla, 2006; Meigs et al., 2011). To this end, we focused on insect patterns at ecoregional and regional scales, and we combined the ADS data with Landsat time series and forest inventory data to map the impacts of MPB and WSB (1) at a finer spatial scale than the homogeneous ADS polygons and (2) in terms of field-estimated tree mortality.

2.2.2. Landsat imagery and LandTrendr disturbance mapping

We used Landsat TM/ETM + imagery from 1984 to 2012 covering all of Oregon and Washington (35 Landsat scenes intersecting

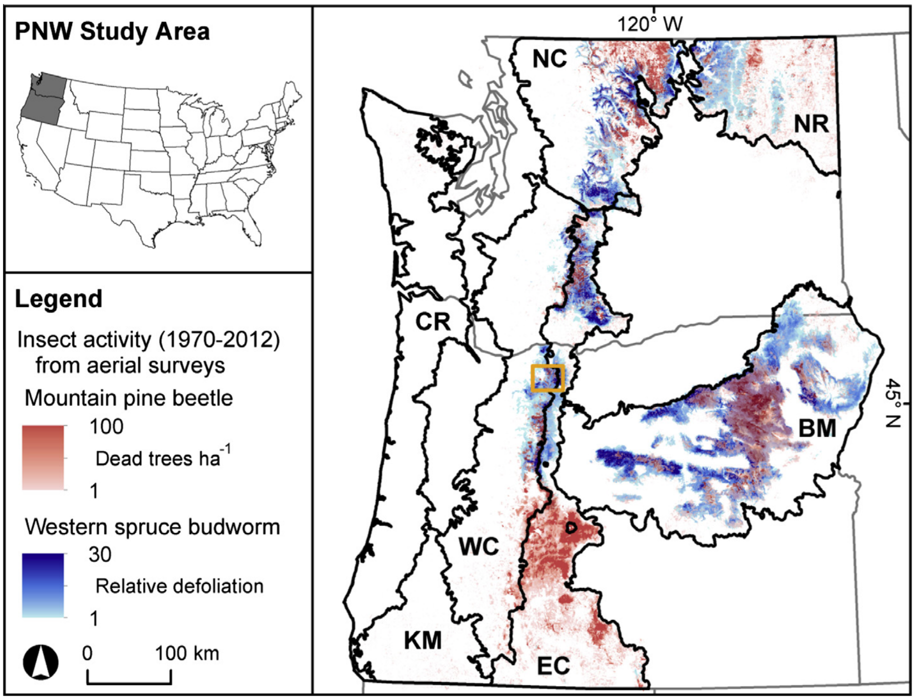

Fig. 1. Study area map. This study focuses on recent activity of mountain pine beetle (MPB) and western spruce budworm (WSB) within the forested ecoregions of the US Pacific Northwest (PNW; Oregon and Washington; inset). Total area of forested ecoregions is ca. 25 M ha, and these two insects have affected ca. 8 M ha according to aerial surveys (1970–2012). Note that aerial surveys characterize MPB in dead trees per unit area and WSB in relative defoliation units. MPB and WSB have been active primarily in the interior mixed-conifer forests and are generally absent in the CR, KM, and much of the WC ecoregions. MPB overlaps WSB activity in this display (MPB shown with 30% transparency), revealing purple locations where both insects have been active. Orange rectangle denotes extent of Fig. 3. Ecoregion (Omernik, 1987) abbreviations: NC: North Cascades; NR: Northern Rockies; CR: Coast Range; BM: Blue Mountains; WC: West Cascades; EC: East Cascades; KM: Klamath Mountains. We assessed only the portions of ecoregions within the two states. (For interpretation of the references to color in this figure legend, the reader is referred to the web version of this article.)

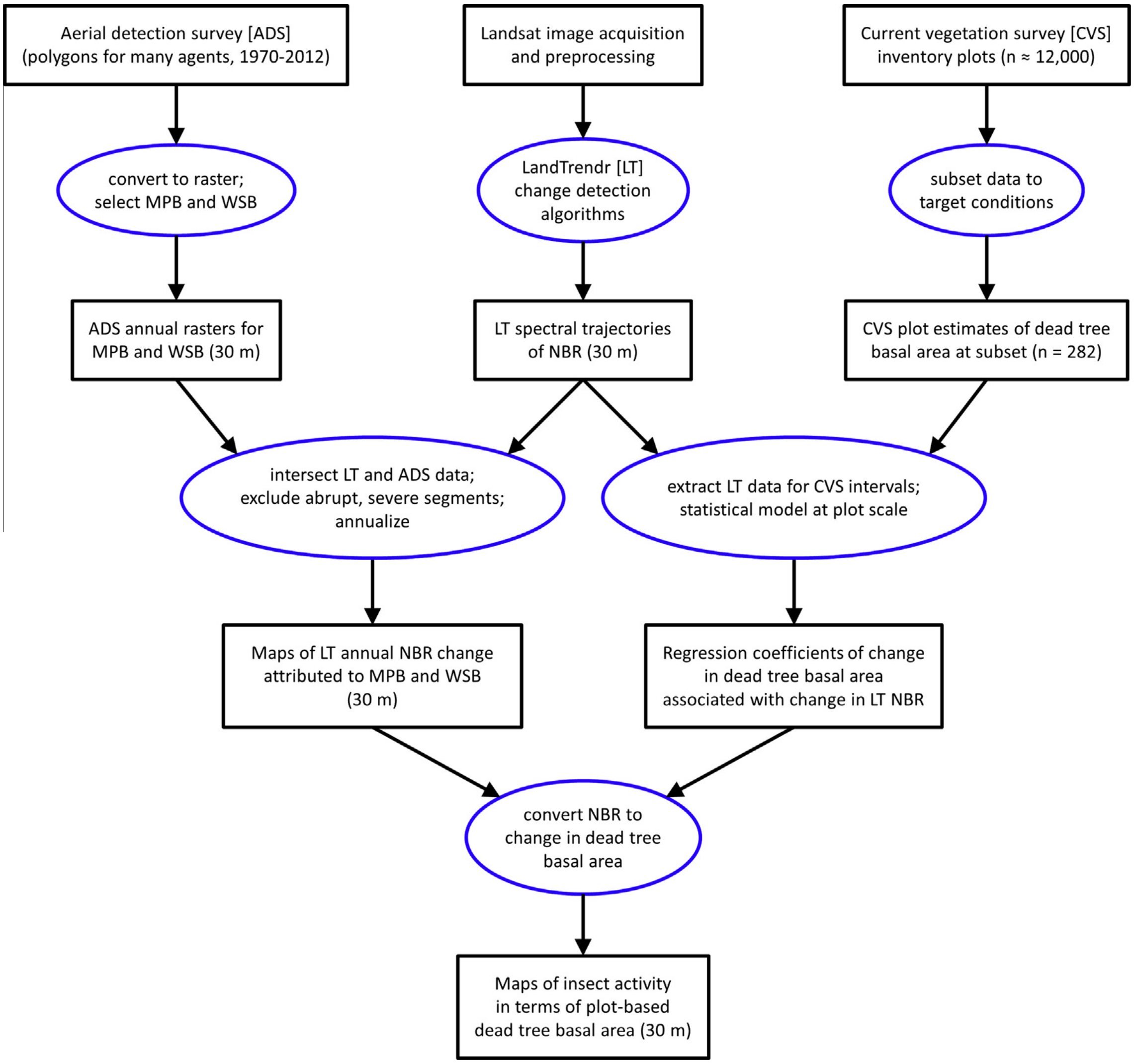

Fig. 2. Datasets and processing steps for Objective 1. See Section 2 for details. Abbreviations: ADS: aerial detection survey; CVS: Current Vegetation Survey; MPB: mountain pine beetle; WSB: western spruce budworm; LT: LandTrendr change detection (Kennedy et al., 2010); NBR: Normalized Burn Ratio (Key and Benson, 2006). Note that at the end of the process there are four sets of annual maps based on two NBR slope thresholds (high, low) and two insects (MPB, WSB).

Worldwide Reference System paths 42–48 and rows 26–31; Appendix A). We applied LandTrendr algorithms and analyses, which are described in detail by Kennedy et al. (2010). Briefly, we downloaded georectified images from the USGS Landsat archive and applied a series of pre-processing, processing, and analysis steps to assess trajectories of change (vegetation decline and growth) associated with disturbance dynamics (Kennedy et al., 2010; Meigs et al., 2011).

Pre-processing involved atmospheric correction using the LEDAPS algorithms (Masek et al., 2006) and cloud masking using the FMASK algorithm (Zhu and Woodcock, 2012), with occasional cloud mask additions following quality control screening. All images were reprojected from the standard USGS UTM projection to the standard US Continental Albers Equal Area projection to allow mosaicking across Landsat scenes. The result was a temporal stack of images with minimal atmospheric and cloud interference, from which we selected the clearest pixel per year near the median date of each stack (generally August 1st) for further analysis.

We then calculated the Normalized Burn Ratio spectral vegetation index (NBR; Key and Benson, 2006), which decreases with forest disturbance and increases with forest growth (Kennedy et al., 2010). By contrasting Landsat bands four (near infrared) and seven (short wave infrared), NBR is similar to spectral indices used in other remote sensing assessments of insect effects (e.g., Wulder et al., 2006; Vogelmann et al., 2009; Goodwin et al., 2010; Meigs et al., 2011; Meddens et al., 2013). NBR is also widely familiar to the fire science community (Eidenshink et al., 2007), and sensitivity analyses have shown its utility for capturing various disturbance dynamics in our study region (Kennedy et al., 2010; Cohen et al., 2010).

Following these pre-processing steps, we applied LandTrendr temporal segmentation algorithms to the NBR time series at the pixel scale (30-m grain). Segmentation distills an often-noisy annual time series into a simplified set of vertices and segments to capture the salient features of a trajectory while omitting most false changes (Kennedy et al., 2010). First, we identified disturbance segments as those where NBR declined between vertices. Then, for each disturbance segment, we mapped the absolute change in NBR as an estimate of disturbance magnitude. We also mapped the onset year, duration (in years), and slope of each segment (where slope is total NBR magnitude of a segment divided by duration). This latter variable – NBR slope – has the potential to distinguish abrupt, severe disturbances like stand-replacing wildfire and logging from more gradual, subtle changes due to insect activity (see Section 2.3.1 below). NBR slope also integrates short-duration, lower magnitude changes associated with some MPB activity with longer-duration, higher magnitude changes associated with WSB activity in more productive forest types (Meigs et al., 2011).

2.2.3. Field-based estimates of tree mortality from forest inventory data

We related LandTrendr-based changes in NBR to concurrent field-based estimates of tree mortality from the federal Current Vegetation Survey (CVS) database. The CVS began as a systematic forest inventory on US Forest Service lands in the PNW (Max et al., 1996) and subsequently was integrated into the national Forest Inventory and Analysis program (Bechtold and Patterson, 2005). Most CVS plots were measured twice, as early as 1993 and as late as 2007 (i.e., intervals vary from one to 14 years). CVS plots are located on a systematic grid (one plot every 2.7 km in non-wilderness, 5.5 km in wilderness; Ohmann et al., 2007) and represent an unbiased sample of Forest Service land. Each CVS plot covers one hectare and includes nested subplots for different vegetation attributes, including live and dead tree species, diameter, and height, land use, stand age, and, via repeat measures, tree growth, mortality, and regeneration. For each CVS measurement, we computed per-unit-area total live and dead tree basal area and density, as well as their absolute and relative changes. Our previous research showed that LandTrendr change detection was most strongly associated with basal area mortality (Meigs et al., 2011), so we used the absolute change in dead tree basal area as our primary estimate of plot-scale tree mortality and response variable in regression modeling (see Section 2.3.2 below).

Because we were interested in capturing insect effects on forest stands during CVS intervals, we subsetted the inventory data in several important ways. Specifically, we focused on CVS plot intervals with these characteristics: aerial detection of MPB or WSB within three years of either measurement (an inclusive interval accounting for potential lagged mortality and/or missed detection), at least 10 measured trees, total tree basal area of at least two units (m^2 ha^{-1}), and a remeasurement interval of at least three years. We also excluded CVS plots with decreasing dead tree basal area (i.e., plots where more tree basal area died before the first observation than during the interval; Azuma, 2010), increasing NBR (i.e., spectral evidence of vegetation growth rather than loss or no change), and evidence of human disturbance within the interval (i.e., $\geqslant 5\%$ of live tree stems removed by human activity). We thus narrowed the sample population substantially from the overall CVS database ($n \approx 12{,}000$) to our final subset ($n = 282$).

We recognized that this subset includes some plots with both MPB and WSB effects as well as other non-anthropogenic disturbances (e.g., other insects, fire, wind) between CVS observations. Rather than further narrowing the database to specific MPB and WSB subsets and excluding locations with potential secondary disturbances, we retained this more general mortality subset to cover a broader range of mortality effects across the region. In addition, by combining both insects in the same mortality subset, we were able to retain a broader scope of inference, calibrate insect damage to a more general biophysical relationship, and compare MPB and WSB maps in consistent units of change.

2.3. New maps of insect impacts on tree mortality

Following the data acquisition, pre-processing, and processing steps described above, we leveraged the aerial surveys, Landsat spectral trajectories, and CVS inventory data to create new maps of MPB and WSB impacts on tree mortality (Fig. 2). All geospatial processing, statistical analyses, and data visualizations were performed with the ArcGIS, IDL, GDAL, Python, or R programs.

2.3.1. Combining Landsat and aerial survey data

First, we identified all Landsat pixels exhibiting a negative change in NBR within locations attributed to MPB or WSB activity by ADS polygons. Then, we defined our initial Landsat-based insect maps by selecting all LandTrendr disturbance temporal segments intersected in at least one year by ADS damage greater than or equal to a baseline cumulative level (0.8 trees ha^{-1} for MPB; three defoliation units for WSB).

Although these pixel-based segments overlapped spatially and temporally with one or more ADS polygons, the change also could have been driven by non-insect disturbance. To resolve this potentially confounding effect, we used the NBR slope variable (LandTrendr segment NBR magnitude divided by duration) to distinguish insect, stand-replacing fire, and logging disturbance thresholds at stratified-random GIS interpretation points, stratifying by insect agent (MPB, WSB) and Landsat scene ($n = 480$; 40 points in six Landsat scenes for each insect; Appendix A). At each point, we evaluated airphoto and Landsat time series data to identify non-insect ($n = 72$) and presumed insect ($n = 408$) disturbances. We then randomly selected two-thirds of the points as training data and used the other one-third for validation. Although MPB and WSB can have differing NBR magnitude and duration distributions (Meigs et al., 2011), we combined the MPB and WSB data for this threshold exercise because their NBR slope distributions were not significantly different ($P > 0.05$; ANOVA; data log-transformed to meet normality and equal variance assumptions).

To identify key thresholds where slope values balanced the omission and commission errors of both non-insect and presumed insect samples, we plotted producer's and user's accuracy curves (Appendix B), repeating this process 10 times and averaging the threshold values to determine a low threshold (NBR slope = 29) and high threshold (NBR slope = 239). We then created two sets of maps by excluding pixels with NBR slope values above each threshold to examine the sensitivity of the final change maps to the thresholds (uncertainty methods below; Section 2.5). Finally, we extracted the annual incremental change from the Landsat-based insect segments (NBR magnitude; Fig. 2), assembled regional mosaics for each year (1984–2012), and derived cumulative disturbance summaries analogous to the ADS cumulative summaries (onset, cumulative magnitude, and count).

2.3.2. Statistical modeling of Landsat- and field-based estimates of change

To relate these maps of Landsat NBR change associated with mountain pine beetle and western spruce budworm to a meaningful, field-based estimate of change, we performed Reduced Major Axis (RMA) regression modeling between Landsat and CVS inventory plot data. RMA regression has several advantages over ordinary least squares or other simple linear approaches, particularly in a remote sensing framework (Cohen et al., 2003). Foremost among these is the symmetry of the variance structure around the RMA fit (i.e., sum of squares are minimized with regard to both the X and Y axes rather than the Y axis only as in OLS regression; Cohen et al., 2003). This symmetry recognizes that both the X and Y variables are measured with error and also enables the interchanging of axes such that either variable can be evaluated on the X or Y axis. Because our specific objective was to create maps of the change in dead tree basal area based on the change in NBR, this simple, symmetrical, univariate approach was optimal.

For each CVS plot, we first extracted the mean annual NBR values within a 13-pixel footprint anchored on the plot's X–Y coordinates (Ohmann et al., 2007). This footprint is analogous to the one hectare CVS sample plot and provides a small buffer for spatial offsets between raster data and CVS plot centers as well as GPS coordinate errors (Zald et al., 2014). We then calculated the change in NBR during the CVS interval and used this as our predictor variable in the RMA regression. Our *a priori* response variable for tree mortality mapping was the change in dead tree basal area ($m^2\ ha^{-1}$) during the CVS interval. This univariate model (change in dead basal area as a function of the change in NBR) performed as well as or better than other potential models with other tree change metrics (live basal area, live and dead tree density) and spectral indices (relative differenced NBR [Miller and Thode, 2007], pre-disturbance and differenced tasseled-cap indices [Crist and Cicone, 1984]; data not shown). To complete the mapping process, we applied the coefficients from this RMA regression to all disturbance segments in the NBR insect maps to derive maps of estimated change in dead tree basal area attributable to MPB and WSB activity in all years (Fig. 2).

2.4. Comparison of recent MPB and WSB activity

For our second objective, we summarized the timing, extent, and cumulative impacts of MPB and WSB across forested ecoregions of the PNW. We compared three different sets of maps – original ADS, Landsat-based low NBR slope threshold, and Landsat-based high NBR slope threshold – for each insect at ecoregional and regional scales. We also combined the map displays with time series of the extent and per-unit-area impacts on estimated tree mortality associated with MPB and WSB. These time series enabled the comparison of the onset, duration, and overall synchrony of outbreaks between the two insect agents and among ecoregions. We hypothesized that widespread synchrony would be evidence of broad, exogenous drivers such as drought, whereas asynchrony would imply independent drivers such as local to ecoregional history of land use and other disturbances.

2.5. Uncertainty analysis

Recognizing that there are important sources of uncertainty throughout our data processing and analysis framework, we evaluated the sensitivity of mapped outputs and relationships at multiple steps in the mapping workflow (Fig. 2). For example, to assess the variability within the ADS polygons, we compared the extent and cumulative damage from the ADS data to the new Landsat-based insect maps (which, by definition, quantify insect damage only within the ADS polygons but at a finer resolution). We also compared the onset year and count (number of years) of the ADS- and Landsat-based maps by differencing the two types of maps where they overlapped in space (i.e., excluding ADS pixels without Landsat change pixels) and time (i.e., 1986–2012, excluding potential confounding effects of the initial Landsat change year [1984–1985]). In addition, we assessed the sensitivity of the insect/non-insect NBR slope threshold by comparing the two sets of Landsat-based maps (high and low slope thresholds) in terms of their extent and cumulative impacts (dead tree basal area). Finally, although we focused on recent MPB and WSB dynamics captured by the ADS, Landsat, and CVS data, many other disturbance processes influence these forests. The impacts of other insects, wildfires, pathogens, logging, drought, and additional factors contribute to the variation in these datasets but are beyond the scope of this study.

3. Results

3.1. New Landsat-based maps of tree mortality associated with insect activity

Focusing on locations identified by aerial surveys of mountain pine beetle and western spruce budworm, our new maps capture insect-associated vegetation change at the Landsat pixel scale (30-m) across the PNW Region. In addition, these maps characterize insect effects in units of tree mortality based on the relationship between Landsat (NBR index) and forest inventory (dead tree basal area) data (Appendix C; RMA regression; $n = 282$; $R^2 = 0.67$). Here, we describe key attributes of these new Landsat-based maps, comparing them to the original aerial survey maps at landscape and regional scales before interpreting the maps to compare the two insects below (Section 3.2).

At the forest landscape scale, the cumulative Landsat-based maps of insect impacts revealed much more fine-grained variability than the cumulative aerial survey polygons (Fig. 3). For both insects, cumulative mortality was highly spatially variable among Landsat pixels (30-m), whereas the ADS polygons were more extensive in space, particularly lower-magnitude WSB defoliation. As expected, the high NBR slope threshold maps (Fig. 3C and D) showed a higher range of mortality and larger cumulative extent than the low NBR slope threshold maps (Fig. 3A and B). The Landsat high NBR slope threshold maps also resulted in the commission of some contemporaneous disturbances (e.g., stand-replacing fire in the MPB high map; Fig. 3C). In contrast, by definition, the low threshold maps omitted these more severe non-insect disturbances but also omitted higher magnitude impacts attributable to insects (i.e., in locations without fire or logging).

Across the PNW Region, comparisons among the ADS and Landsat-based maps illustrate some key similarities in onset year and differences in number of years mapped (Appendix D). Regarding onset (i.e., the first year of insect activity), there was high correspondence between the ADS and Landsat maps, with a large spike at zero difference indicating that the first year of insect-caused change was identical in both maps (Appendix D). In contrast, the negative distributions of the difference between the ADS and Landsat count (i.e., number of years mapped) showed that the Landsat maps captured change in more years than the ADS maps during years of mutual coverage (1986–2012; Appendix D). For both insects, annual counts were highest close to zero (i.e., no difference in number of years), although both insects exhibited a small increase near -25 years, suggesting the presence of some relatively long-duration Landsat disturbance segments (Appendix D). Finally, the Landsat high and low NBR slope threshold maps were similar across most of the range of count difference but diverged close to zero, as expected, because the low threshold maps exclude relatively short-duration, severe disturbance segments.

3.2. Landscape and regional comparisons of MPB and WSB timing, extent, and cumulative impacts

Across forested ecoregions of the PNW, although there was high variability in insect activity and impacts, spatiotemporal patterns were evident in both the aerial survey- and Landsat-based maps. Because MPB and WSB were negligible in the Coast Range and Klamath Mountains (Fig. 1), we exclude those ecoregions from the following results and discussion.

3.2.1. Recent insect timing and extent

MPB outbreaks occurred in two distinct phases according to ADS data (Fig. 4). An early phase of activity initiated in the Blue Mountains and East Cascades of Oregon during the 1970s and 1980s, respectively. These were the most extensive MPB outbreaks, approaching 10% of the East Cascades ecoregion at the mid-1980s peak (Fig. 4F) and exceeding 2 M cumulative ha in each of these ecoregions (according to ADS data; Appendix E). A second wave of MPB activity occurred throughout the PNW after the year 2000, affecting dry forests in all of the ecoregions except for the Blue Mountains, where MPB had been widespread 30 years earlier according to the ADS. These latter outbreaks appeared to be synchronous across ecoregions, potentially driven by exogenous

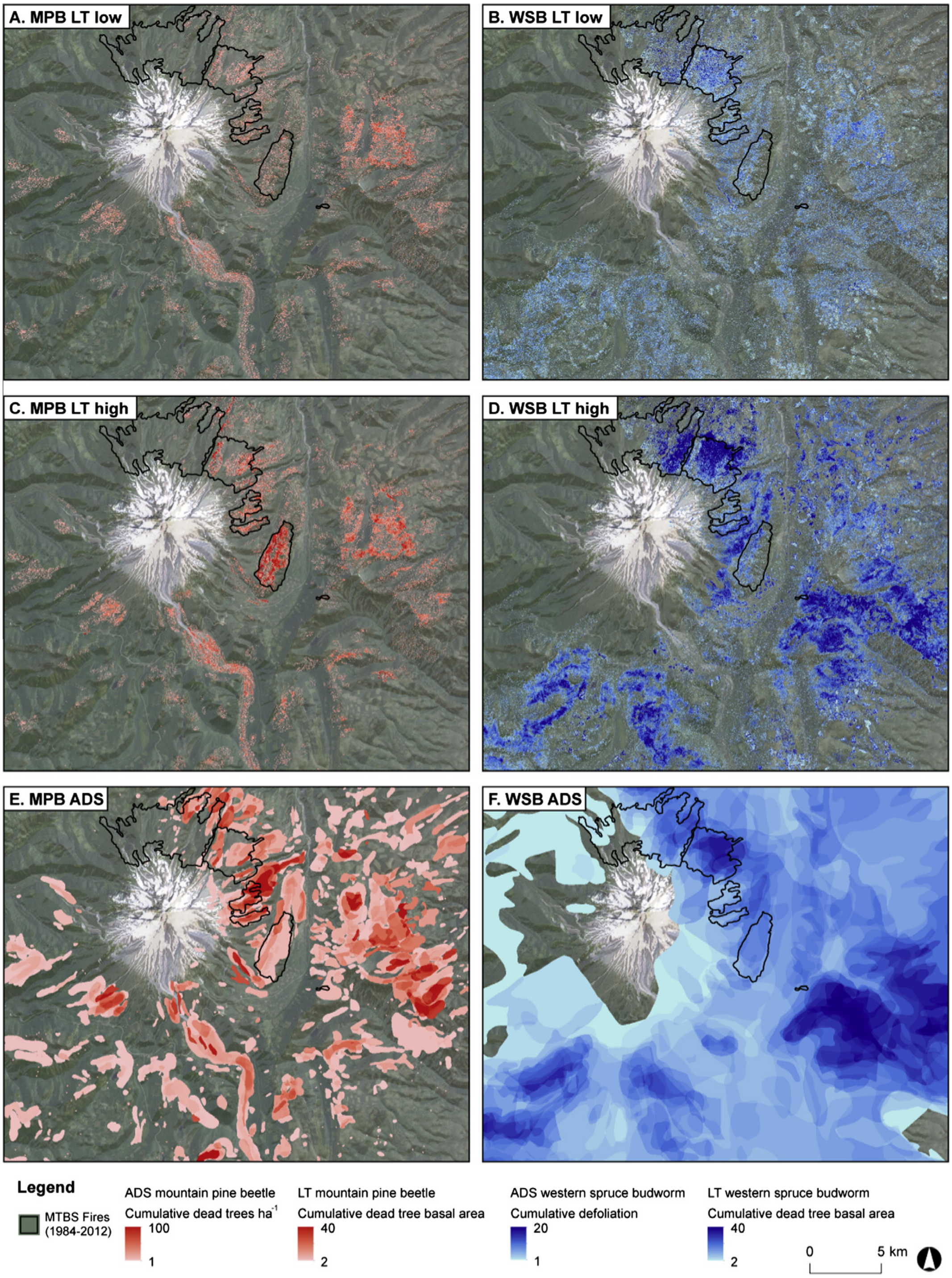

Fig. 3. Example landscape maps comparing cumulative impacts (1984–2012) of mountain pine beetle (MPB; red) and western spruce budworm (WSB; blue) according to aerial detection surveys (ADS) (E, F) and two thresholds of LandTrendr (LT). This Mt. Hood area has representative examples of both insects in a centrally located landscape (Fig. 1). Fire perimeters from Monitoring Trends in Burn Severity (MTBS) show potential for fires to be included in insect maps at the high LT NBR slope threshold. Note that LT insect maps are constrained within ADS polygons but exhibit finer-grained detail and change estimates in consistent tree mortality units. Aerial surveys characterize MPB in dead trees per unit area and WSB in relative defoliation units. Base maps: World Terrain Base and ESRI Imagery World 2D from http://server.arcgisonline.com. (For interpretation of the references to color in this figure legend, the reader is referred to the web version of this article.)

factors such as regional climate (e.g., drought-stressed host trees). At the regional scale, MPB outbreaks did not exceed 1% of the PNW in any given year (Fig. 4A).

WSB extent exceeded MPB extent in all ecoregions except for the East Cascades, where the interannual and cumulative extents were similar according to ADS data (Fig. 4, Appendix E). Reflecting differences in epidemiology and host susceptibility, WSB outbreaks first appeared in the North Cascades of Washington in the 1970s. WSB emerged in other ecoregions during the 1980s, first in the Blue Mountains and Northern Rockies ecoregions and subsequently in the East and West Cascades, returning to the North Cascades of Washington during the 1990s and 2000s (Fig. 4). Although there was some WSB activity in other dry forest ecoregions, the WSB outbreak that initiated in the Blue Mountains ecoregion in

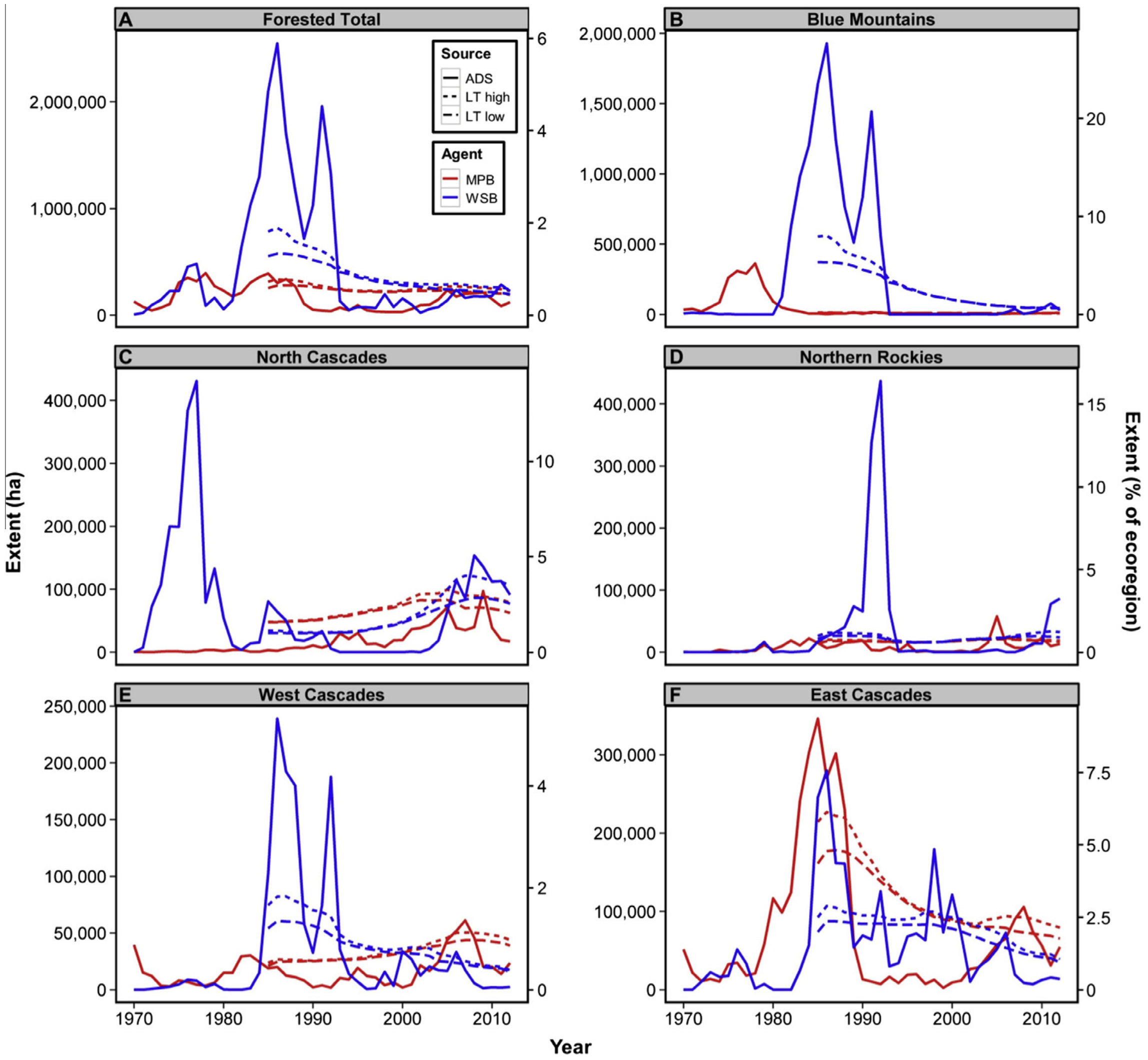

Fig. 4. Temporal patterns of extent (ha and percent of ecoregion) of recent mountain pine beetle (MPB; red) and western spruce budworm (WSB; blue) activity according to aerial detection surveys (ADS; 1970–2012) and two thresholds of LandTrendr change detection (LT; 1984–2012) across forested ecoregions of the PNW. LT high refers to the high NBR slope threshold; LT low refers to the low NBR slope threshold (see Section 2.3.1). Note that ADS extent is the affected area associated with polygons, whereas LT extent is the vegetation change area associated with pixels. We calculate the "Forested Total" across all ecoregions but do not show the Coast Range and Klamath Mountains ecoregions here due to the absence of MPB and WSB activity. Note that the *Y* axes vary by ecoregion. See Appendix E for cumulative extent. See Figs. 1 and 5 for regional spatial patterns. (For interpretation of the references to color in this figure legend, the reader is referred to the web version of this article.)

the 1980s and appeared to spread into the East and West Cascades was the most extensive insect outbreak in the regional record (Fig. 4). According to the ADS, that outbreak exceeded 25% of the Blue Mountains ecoregion (ca. 12 M cumulative ha; Fig. 4B, Appendix E) and 5% of the PNW Region at its peak (Fig. 4A).

Where they overlapped temporally (after 1984), the Landsat- and ADS-based time series of outbreak extent exhibited similar temporal patterns, but the Landsat-based maps were much smoother from year to year, illustrating stability associated with lasting vegetation change (Fig. 4, Appendix E). In contrast, the ADS maps covered more years (back to 1970) but showed much larger interannual variability, demonstrating higher uncertainty due in part to sporadic observations as well as the ADS focus on the current year's affected area rather than multiple years of durable change.

Although the Landsat high NBR slope threshold maps were more extensive than the low threshold maps by definition, the differences were small relative to the difference between the ADS and Landsat maps (Fig. 4, Appendix E). We thus displayed the high NBR slope threshold in a regional map (Fig. 5) to compare spatial patterns of insect activity and cumulative impacts with the ADS-based record (Fig. 1). As with the landscape-scale example (Fig. 3), the regional Landsat-based maps exhibited finer-grained impacts and substantially reduced overall extent (Fig. 5).

3.2.2. MPB and WSB impacts on tree mortality

By accounting for the impacts of both MPB and WSB in the same disturbance units (basal area mortality), the Landsat-based mortality maps facilitated comparisons among agents and ecoregions that were not possible with the Landsat-based extent estimates or with the ADS data alone (Figs. 4–6). Specifically, although the temporal patterns were similar between the Landsat-based extent and tree mortality estimates, the mortality maps demonstrated higher interannual variability (Figs. 4 and 6). For example, in the East Cascades, WSB resulted in higher total tree mortality than MPB for several years around the year 2000 (according to the Landsat high NBR slope threshold; Fig. 6F), a pattern not evident in the Landsat extent data (Fig. 4F) or in cumulative mortality trajectories (Appendices E and F). In addition, by explicitly quantifying per-unit-area insect impacts, the Landsat mortality maps showed that WSB exceeded MPB not only in cumulative extent but also in

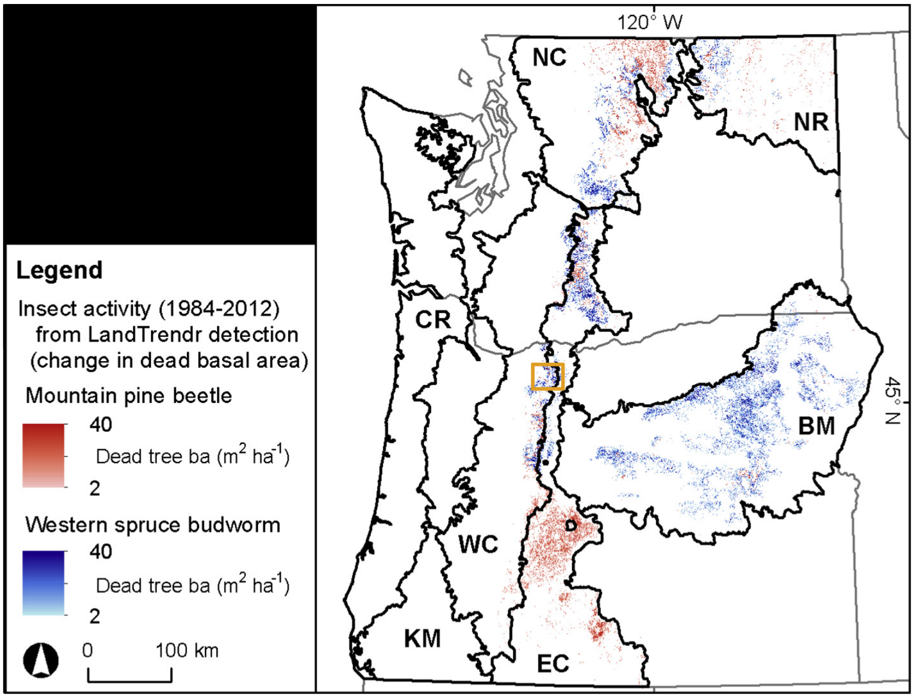

Fig. 5. Spatial patterns of cumulative insect effects on tree mortality (dead tree basal area; 1984–2012) from LT high slope threshold maps across the PNW. Mountain pine beetle (MPB; red) overlaps western spruce budworm (WSB; blue) activity in this display, and both insects are much less extensive here than in the analogous aerial survey-based maps (Figs. 1 and 4). Note the absence of MPB and WSB in the CR, KM, and most of the WC ecoregions. Orange rectangle denotes extent of Fig. 3. Temporal patterns shown in Fig. 6. Ecoregion (Omernik, 1987) abbreviations: NC: North Cascades; NR: Northern Rockies; CR: Coast Range; BM: Blue Mountains; WC: West Cascades; EC: East Cascades; KM: Klamath Mountains. We assessed only the portions of ecoregions within the two states. (For interpretation of the references to color in this figure legend, the reader is referred to the web version of this article.)

cumulative total tree mortality across most ecoregions (Appendices E and F).

Across the PNW Region, interannual tree mortality associated with WSB exceeded MPB-associated mortality from 1985 to 2002, and the two insects resulted in similar total tree mortality for the last 10 years of the Landsat record (2003–2012; Fig. 6A). As expected due to the previously described extent patterns, about 75% of regional WSB impacts occurred in the Blue Mountains (Fig. 6B). The earlier peak in MPB-associated mortality occurred largely in the East Cascades, whereas the later peak occurred in all ecoregions except for the Blue Mountains (Fig. 6). Although patterns of cumulative tree mortality were similar between the two insects, the WSB low threshold exceeded the MPB high threshold estimate of cumulative tree mortality in three out of the five ecoregions; cumulative mortality associated with MPB outbreaks was higher only in the East Cascades (Appendix F).

4. Discussion

4.1. Key aspects of new Landsat-based insect atlas

Our Landsat-based insect atlas complements existing ADS maps in three important ways, thereby enhancing the ecological resolution for analysis, interpretation, and management of insect impacts. Specifically, the Landsat-based maps (1) capture variation of insect impacts at a finer scale (30 m) within ADS polygons, substantially reducing estimated insect extent; (2) provide consistent estimates of change for multiple agents, particularly long-duration changes; (3) quantify change in terms of field-measured tree mortality (dead basal area) for a bark beetle and defoliator. Because they are derived from three complementary datasets that span the PNW Region (aerial detection surveys, Landsat time series, forest inventory plots), these new maps facilitate comparisons across space, time, and insect agents that have not been possible to date.

At the forest landscape scale, the fine-grained, Landsat-based insect maps highlight the coarse-scale uncertainties in the ADS polygons, particularly the low damage polygons (Fig. 3). For western spruce budworm, the much larger ADS extent is evident in all ecoregions (Figs. 3 and 4). This result – as well as the negative distribution of differences in count (number of years) across the region (Appendix D) – illustrates the biophysical contrast between transient defoliation detected by ADS observers versus the lasting vegetation impacts identified by the Landsat time series. The more durable changes quantified by the Landsat trajectories have important implications for vegetation succession, fuel profiles, and carbon, nutrient, and hydrological cycling.

At the regional scale, the Landsat-based maps substantially reduce the extent and cumulative impacts estimated from the ADS maps (Figs. 1, 4 and 5, Appendix E), demonstrating the potential to overestimate insect damage from ADS polygons without recognizing that they include some live trees. We suggest that whereas the ADS polygons represent a useful coarse filter to track short-term insect activity, the Landsat trajectories provide a fine filter to identify actual, long-term insect impacts while characterizing the variability within ADS polygons. In this way, Landsat-based maps help to resolve how the ADS maps appear to overestimate regional-scale insect extent while simultaneously underestimating stand-scale effects (Meigs et al., 2011; Meddens and Hicke, 2014). Researchers and forest managers could use both types of maps to identify locations across the region where MPB and WSB are currently active (ADS polygons) and precisely where they have had especially severe, cumulative impacts (Landsat trajectories).

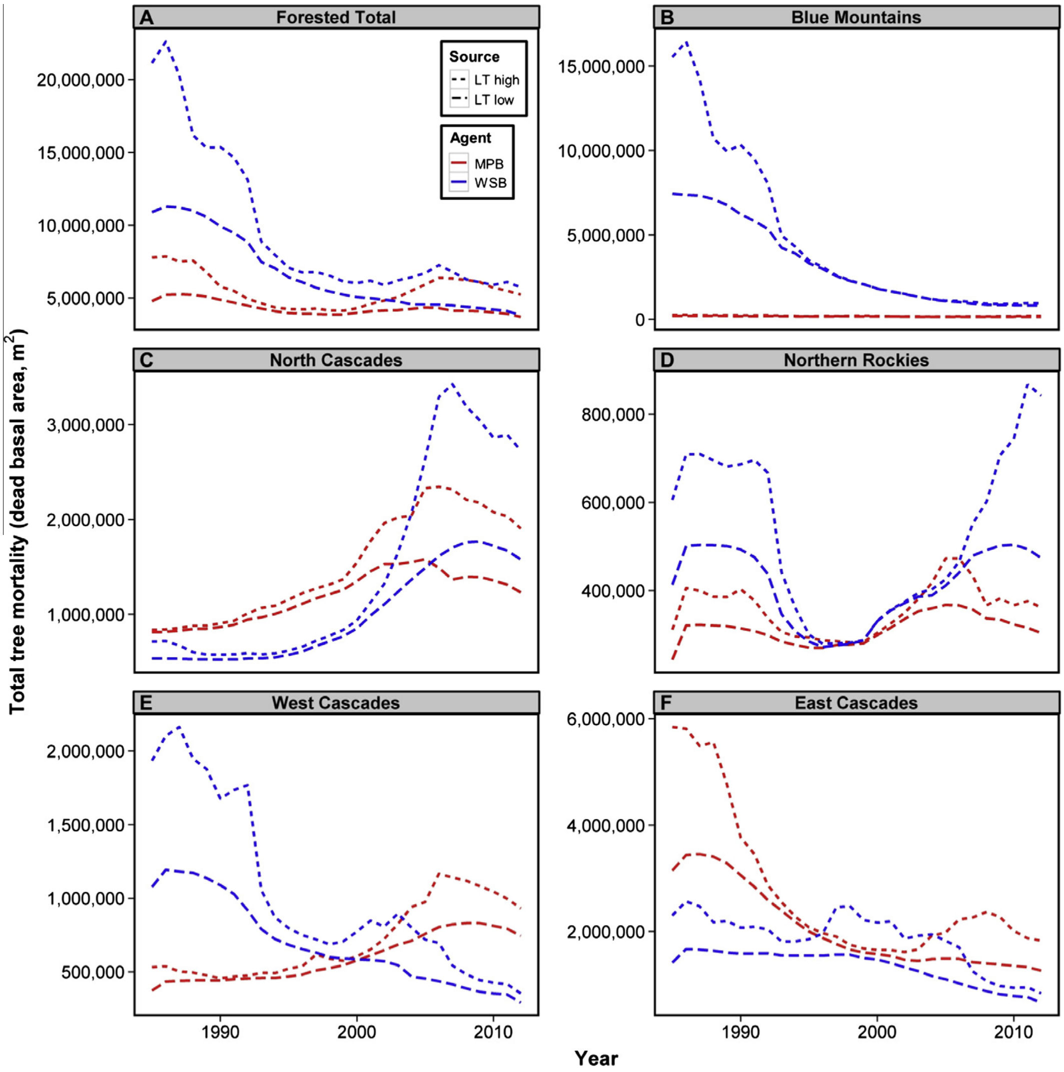

Fig. 6. Temporal patterns of mountain pine beetle (MPB; red) and western spruce budworm (WSB; blue) effects on tree mortality (total dead basal area) from LandTrendr change detection (LT; 1984–2012) across forested ecoregions of the PNW. LT high refers to the high NBR slope threshold; LT low refers to the low NBR slope threshold (see Section 2.3.1). We calculate the "Forested Total" across all ecoregions but do not show the Coast Range and Klamath Mountains ecoregions here due to the absence of MPB and WSB activity. Note that the *Y* axes vary by ecoregion. Spatial patterns of LT high threshold data shown in Fig. 5. Cumulative effects shown in Appendix F. (For interpretation of the references to color in this figure legend, the reader is referred to the web version of this article.)

Previous mapping studies have focused primarily on MPB and other bark beetle outbreaks, leveraging either ADS (e.g., Williams and Birdsey, 2003; Meddens et al., 2012; Preisler et al., 2012) or Landsat data (e.g., Wulder et al., 2006; Goodwin et al., 2010; Meddens and Hicke, 2014). To our knowledge, this study is the first to capture both bark beetle and defoliator impacts in an integrated mapping framework, combining complementary remotely sensed and ground-based data to render fine-grained maps of insect impacts on tree mortality at a regional scale. It is also the first study to quantify and compare MPB and WSB impacts across the US PNW Region.

4.2. Regional spatiotemporal patterns of MPB and WSB impacts

MPB outbreaks exhibited both landscape-scale asynchrony (in the early outbreaks) and regional-scale synchrony (in the late outbreaks). The former affected much more area in the PNW, creating a large pulse of tree mortality and setting the stage for potential interactions with subsequent wildfires (Hicke et al., 2012). The latter may be particularly important in the context of global change and broader insect-climate dynamics across western North America (Raffa et al., 2008; Meddens et al., 2012).

Recent MPB outbreaks have been the subject of intense scientific and public concern, particularly the regional-scale outbreaks in British Columbia and US Rocky Mountains (e.g., Meddens et al., 2012). Although less prominent, recent MPB outbreaks in the PNW have affected a substantial proportion of the ecoregions where host trees (lodgepole pine) are present (Fig. 4), resulting in widespread tree mortality (Figs. 5 and 6). Preisler et al. (2012) quantified MPB outbreaks in OR and WA, attributing recent activity (ADS dead tree estimates at the km^2 scale) to beetle pressure and climate drivers. Our MPB time series data are consistent with the aerial survey-based summaries of Preisler et al. (2012) but focus on ecoregional rather than statewide summaries, as well as the lasting, cumulative impacts on tree mortality due to bark beetles and defoliators. Our fine-grained mortality maps have the potential to aid future analyses of the drivers of MPB and WSB outbreaks – including insect population dynamics, climate, and land use history – from forest stand to regional scales.

Despite the dominance of MPB studies in recent literature on insect outbreaks and mapping, our maps confirm that WSB is a very important disturbance agent across the PNW Region. Whereas

MPB outbreaks are limited to areas with substantial lodgepole pine, WSB outbreaks affect a variety of host tree species, including true firs, spruce, and Douglas-fir (Sanders et al., 1985; Goheen and Willhite, 2006). Due in part to host tree distribution and land use history (Hessburg et al., 2000), WSB extent exceeds MPB extent in all ecoregions except for the East Cascades, where cumulative extents have been similar (Fig. 4, Appendix E). Indeed, the 1980s WSB outbreak in the Blue Mountains dominates the regional record, accounting for much of the insect extent and mortality impacts across all forested ecoregions (Figs. 4 and 6). Although the Landsat-based annual and cumulative MPB impacts initially exceed WSB impacts in the North Cascades (Fig. 6C, Appendix F), this is the result of the Landsat record beginning after a widespread earlier WSB outbreak (Fig. 4C, Appendix E). Subsequent WSB impacts in the North Cascades exceed MPB impacts, resulting in very similar cumulative mortality by the end of the Landsat record (Fig. 6C, Appendix F) and highlighting the importance of repeat defoliation events in WSB-prone forests (Flower et al., 2014). These complex WSB and MPB dynamics in the North Cascades – and indeed in all ecoregions – illustrate the importance of accounting for both types of insects, as well as incorporating as many years as possible in future analyses.

4.3. Uncertainties and future work

This study advances insect mapping methods by combining aerial, satellite, and field datasets in a novel, regional framework. Though spatially and temporally extensive, the datasets we used have particular strengths and weaknesses (e.g., Meigs et al., 2011; Meddens and Hicke, 2014), underscoring the need to incorporate multiple, complementary sources of data. Specifically, our approach benefits from the use of ADS polygons for attribution/detection of specific insect agents, Landsat time series for fine-grained, consistent change estimates, and CVS field plots for tree mortality estimates. Nevertheless, many uncertainties remain.

Although this assessment is unprecedented in terms of capturing the annual and cumulative impacts of multiple insects from forest stand to regional scales, it extends only to 1984 for the Landsat-based maps and to 1970 for the ADS-based maps. Recent research demonstrates the potential to extend Landsat time series back to 1972 with MSS data (Pflugmacher et al., 2012), which would enable further comparisons of Landsat and ADS data, as well as the capture of additional insect impacts. Longer-term studies based on tree ring data are vital to assess multiple outbreaks and to compare outbreak trends over time (e.g., Swetnam and Betancourt, 1998; Flower et al., 2014). Similarly, although the PNW is a broad, heterogeneous region with many similarities to other regions (e.g., US Rocky Mountains), the datasets we used may not be as readily available or spatiotemporally consistent elsewhere (Meddens et al., 2012). Future studies thus should investigate the integration of applicable aerial, satellite, and field datasets in other regions.

In addition, we focused on the two most prevalent insects in the study region (MPB and WSB), but forests of the PNW are influenced by numerous other disturbance agents, including other insects (e.g., fir engraver beetle [*Scolytus ventralis* LeConte {Coleoptera: Curculionidae}], Douglas-fir tussock moth [*Orgyia pseudotsugata* {McDunnough} {Lepidoptera: Lymantriidae}]; Goheen and Willhite, 2006), wildfire, diseases, logging, and climate change, among others. Future studies could apply our mapping methods to these other disturbances to determine their relative importance while also considering them in a comprehensive attribution analysis. Because our high NBR slope threshold resulted in commission of some non-insect disturbances, and our low NBR slope threshold omitted some insect disturbances (Fig. 3), we suggest that they represent an appropriate range of high and low confidence for insect damage (with the high NBR slope threshold being preferable for visual display at ecoregional and regional scales). These tradeoffs between the high and low NBR slope thresholds also indicate that attribution based solely on spectral change collocated with ADS polygons may be insufficient. Future studies could incorporate ancillary data on other disturbance types (e.g., fire and logging inventories) and spatial patterns (e.g., patch size and shape), as well as known insect drivers such as drought stress and host tree distribution and structure. It is particularly challenging to differentiate the effects of insects alone versus the combined effects of insect outbreaks and management actions, as both insects and humans effectively thin forest stands. Although we excluded CVS inventory plots with evidence of anthropogenic disturbance from our basal area mortality model, our approach still includes pixels within ADS polygons that may have experienced thinning and/or salvage harvest, management responses that have been typical in the study area (e.g., Waring et al., 1992; Azuma, 2010). Finally, our approach limited the Landsat-based maps to pixel trajectories intersected in at least one year by ADS polygons; future work could include disturbance pixels outside of those locations, as well as post-disturbance spectral recovery trajectories (Kennedy et al., 2010; Meigs et al., 2011).

4.4. Management implications

This regional-scale assessment provides unique insights regarding the spatiotemporal patterns of recent bark beetle and defoliator outbreaks, informing potential forest management actions in the US Pacific Northwest. Specifically, our Landsat-based insect maps quantify mountain pine beetle and western spruce budworm impacts on interannual and cumulative tree mortality at a fine spatial scale (30 m), seamlessly across space and time. In recent decades, both native insects have had pervasive yet variable impacts across the dry, interior conifer forests of Oregon and Washington, influencing current forest composition, structure, and function across multiple historic disturbance and management regimes. By identifying where and when each insect has resulted in substantial tree mortality, our maps provide a key context for landscape- and regional-scale strategic planning, ecosystem monitoring, and silvicultural prescriptions.

In addition, by capturing the effects of multiple insect species and constraining maps to locations where substantial tree mortality has occurred, our analysis identifies particular hotspots where bark beetles and defoliators have rendered synergistic impacts. These mixed-conifer forest stands and landscapes, particularly in the Blue Mountains, East Cascades, and North Cascades ecoregions, may warrant special management attention. Recent insect outbreaks in these forests also may amplify the need for proactive landscape restoration (Hessburg et al., 2000), potentially at an increasing pace and scale (Haugo et al., 2015).

Finally, our insect atlas provides an essential baseline against which to measure future changes in forest health. Although widespread, these insects have not affected all potential host forests across the PNW – including Douglas-fir forests in western Oregon and Washington – and future outbreaks could exhibit unprecedented extent or impacts associated with global change. In this context, a particularly critical management concern is the role that insect outbreaks might play in subsequent fire likelihood or severity (Hicke et al., 2012). Indeed, both insects and wildfires are projected to increase in importance in western North American forests (e.g., Bentz et al., 2010; Littell et al., 2010). Given their recent history and likely future dynamics, the accurate assessment and monitoring of these native disturbances will continue to be crucial for sustainable ecosystem management.

Acknowledgements

This research was supported in part by NASA Headquarters under the NASA Earth and Space Science Fellowship Program – Grant NNX11AM01H – and the USDA Forest Service, Forest Health Monitoring (FHM) Evaluation Monitoring – Grant No. WC-F-09-2. We acknowledge Justin Braaten, Kevin Briggs, John Campbell, Julie Johnson, Helen Maffei, Trevor McWilliams, Andrew Merschel, Ariel Muldoon, Matthew Reilly, Heather Roberts, Keith Sprengel, Elizabeth Willhite, Zhiqiang Yang, and Harold Zald for help with data access, analysis, and interpretation. We thank G. Kohler for help with insect taxonomy and the many PNW staff and contractors for collecting and compiling the aerial survey and forest inventory databases. We are grateful to Tiffany Garcia, James Johnston, Jono Meigs, David Shaw, and two anonymous reviewers for their insightful comments. The development and testing of the LandTrendr algorithms reported in this paper were made possible with the support of the USDA Forest Service Northwest Forest Plan Effectiveness Monitoring Program, the North American Carbon Program through grants from NASA's Terrestrial Ecology, Carbon Cycle Science, and Applied Sciences Programs, the NASA New Investigator Program, the Office of Science (BER) of the U.S. Department of Energy, and the following Inventory and Monitoring networks of the National Park Service: Southwest Alaska, Sierra Nevada, Northern Colorado Plateau, and Southern Colorado Plateau.

Appendix A

See Fig. A1.

Appendix B

See Fig. B1.

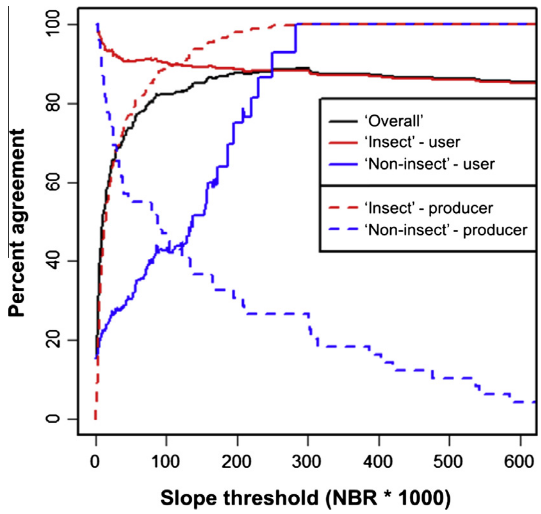

Fig. B1. Example of accuracy thresholds for simple attribution of presumed 'insect' (red) and 'non-insect' (blue) LandTrendr disturbance segments intersected by aerial survey polygons. Note that 'overall' (black) classification accuracy is sensitive to imbalanced sample size. The low slope threshold (29) is defined as the intersection of the two producer's accuracy curves and includes only lower slope values in the insect class. The high slope threshold (239) is defined as the intersection of the two user's accuracy curves and includes many more segments. Final thresholds were averaged from 10 iterations where 2/3 of the sample set ($n = 320$) was used for training and 1/3 ($n = 160$) for validation. See Section 2.3.1 for details. (For interpretation of the references to color in this figure legend, the reader is referred to the web version of this article.)

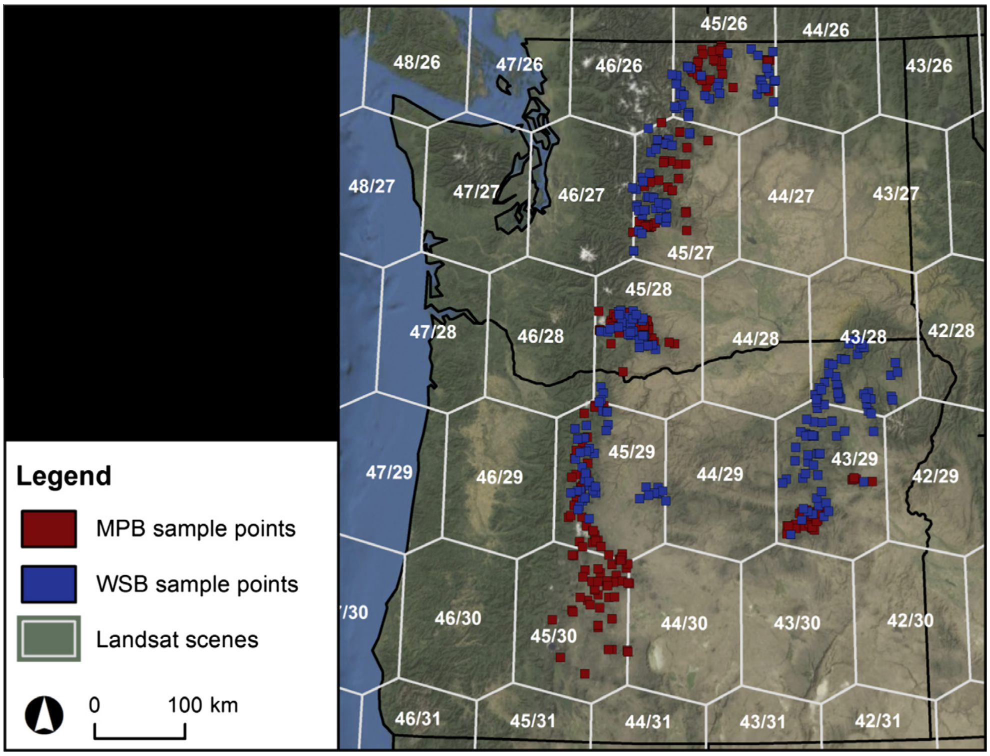

Fig. A1. Map of stratified-random sample points in selected Landsat path/row scenes with mountain pine beetle (MPB; red) or western spruce budworm (WSB; blue) activity according to aerial surveys across the PNW. For each insect, we assessed 40 points in six scenes ($n = 480$ across seven total scenes because one scene had only MPB and one scene had only WSB). At each point, we evaluated airphoto and Landsat time series data for evidence of insect and non-insect disturbance to develop high and low NBR slope thresholds for inclusion in the final Landsat-based maps (Appendix B). See Section 2.3.1 for details. 35 Theissen scenes (polygons accounting for scene overlap) are intersected by OR or WA. Base maps: World Terrain Base and ESRI Imagery World 2D from http://server.arcgisonline.com. (For interpretation of the references to color in this figure legend, the reader is referred to the web version of this article.)

Appendix C

See Fig. C1.

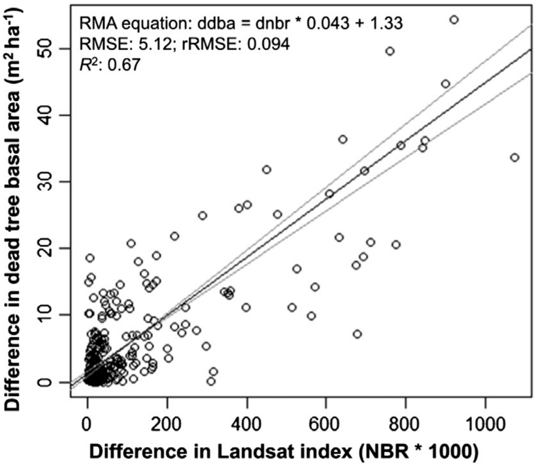

Fig. C1. Plot-scale relationship between LandTrendr-based spectral change (time 1 – time 2) and concurrent field-based dead tree basal area change (RMA regression line with 95% CI). Note that although the regression model fit is weaker at very low levels of change, our objective was to quantify field-based changes associated with substantial, detectable levels of Landsat change. For example, a relatively low scaled NBR difference (100) is equivalent to a relatively modest increase of dead basal area (ca. 5 m^2 ha^{-1}). See Section 2.2.3 for criteria used to subset CVS inventory plots from the overall database ($n \approx$ 12,000) to this refined sample focusing on disturbance associated with MPB or WSB activity according to aerial surveys (n = 282).

Appendix D

See Fig. D1.

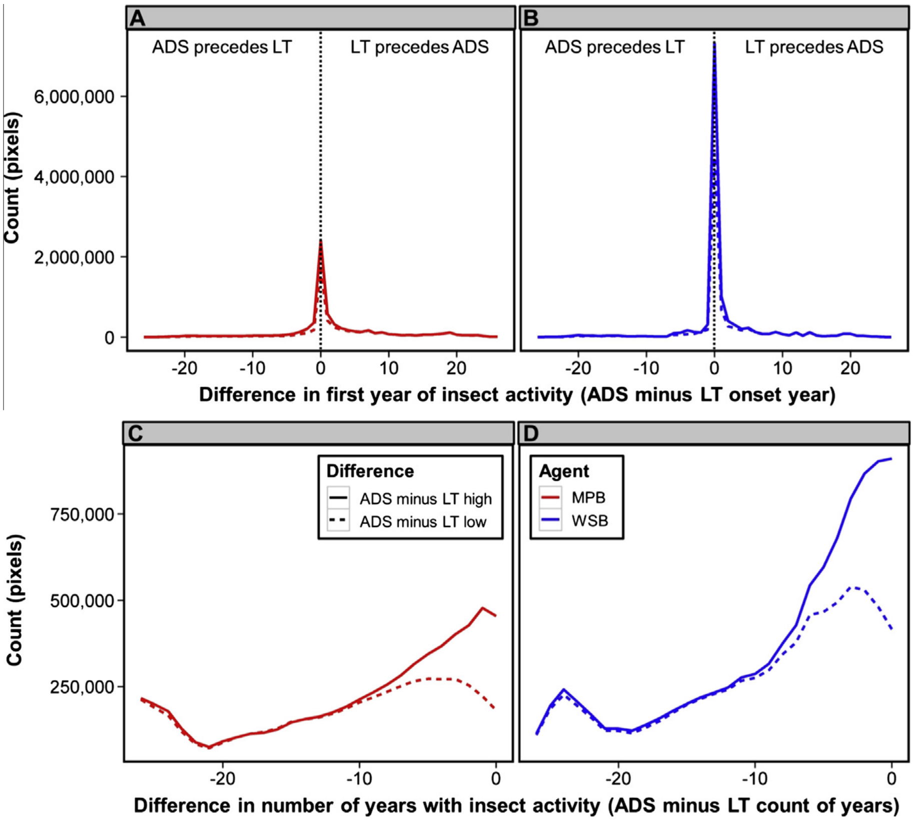

Fig. D1. Difference of insect onset year and count among aerial detection survey (ADS) and LandTrendr (LT) maps of MPB (A and C; red) and WSB (B and D; blue). These comparisons exclude locations with ADS detection only as well as the first year of the Landsat time series (1984–1985), thereby focusing on locations and years of mutual coverage (1986–2012 in both data sources). LT high refers to the high NBR slope threshold; LT low refers to the low NBR slope threshold (see Section 2.3.1). (For interpretation of the references to color in this figure legend, the reader is referred to the web version of this article.)

Appendix E

See Fig. E1.

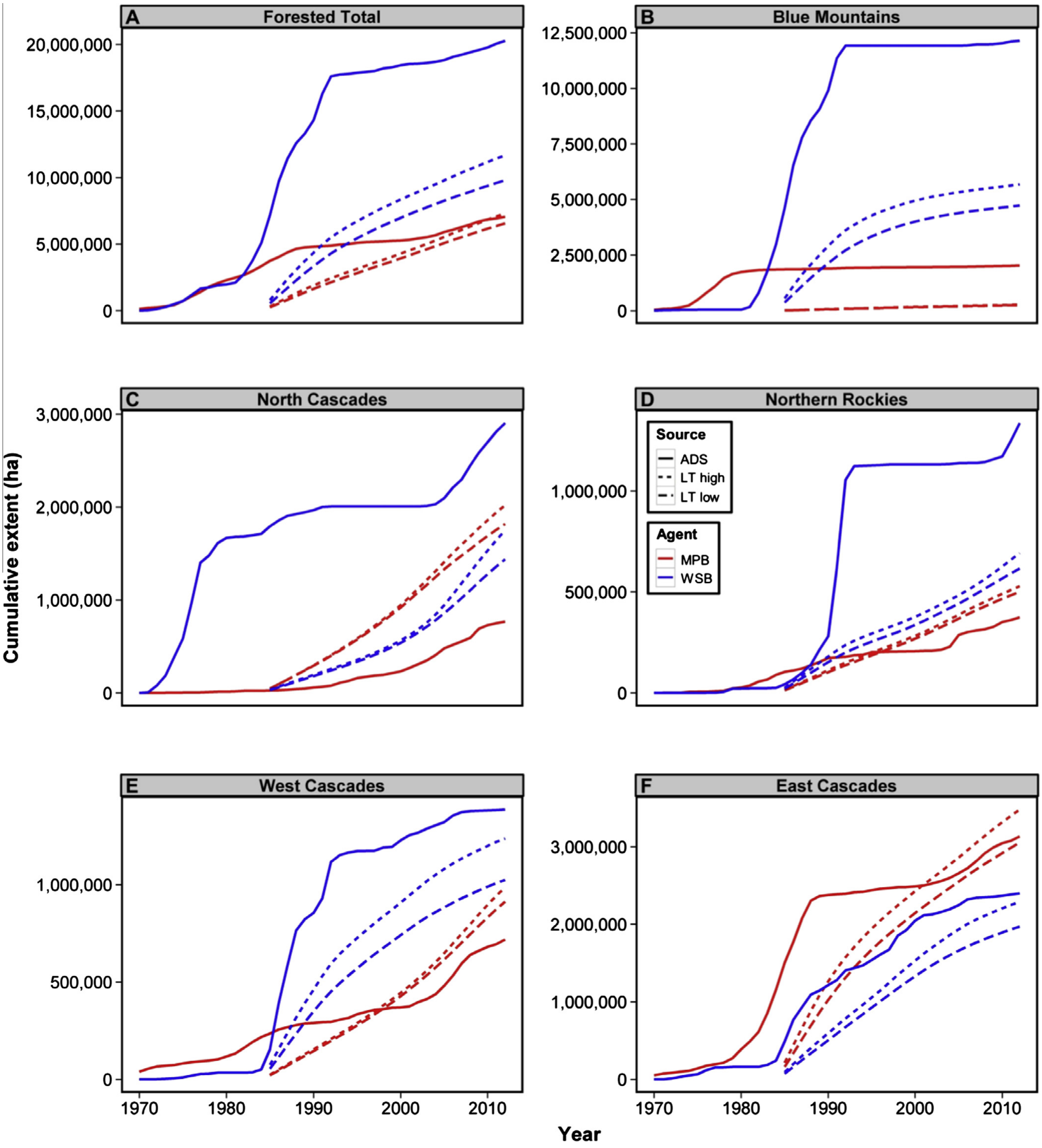

Fig. E1. Cumulative extent (ha) of recent mountain pine beetle (MPB; red) and western spruce budworm (WSB; blue) activity according to aerial detection survey (ADS; 1970–2012) and two thresholds of LandTrendr change detection (LT; 1984–2012) across forested ecoregions of the PNW. LT high refers to the high NBR slope threshold, and LT low refers to the low NBR slope threshold (see Section 2). We calculate the "Forested Total" across all ecoregions but do not show the Coast Range and Klamath Mountains ecoregions here due to the absence of MPB and WSB activity. Note that the *Y* axes vary by ecoregion. Annual effects shown in Fig. 4. (For interpretation of the references to color in this figure legend, the reader is referred to the web version of this article.)

Appendix F

See Fig. F1.

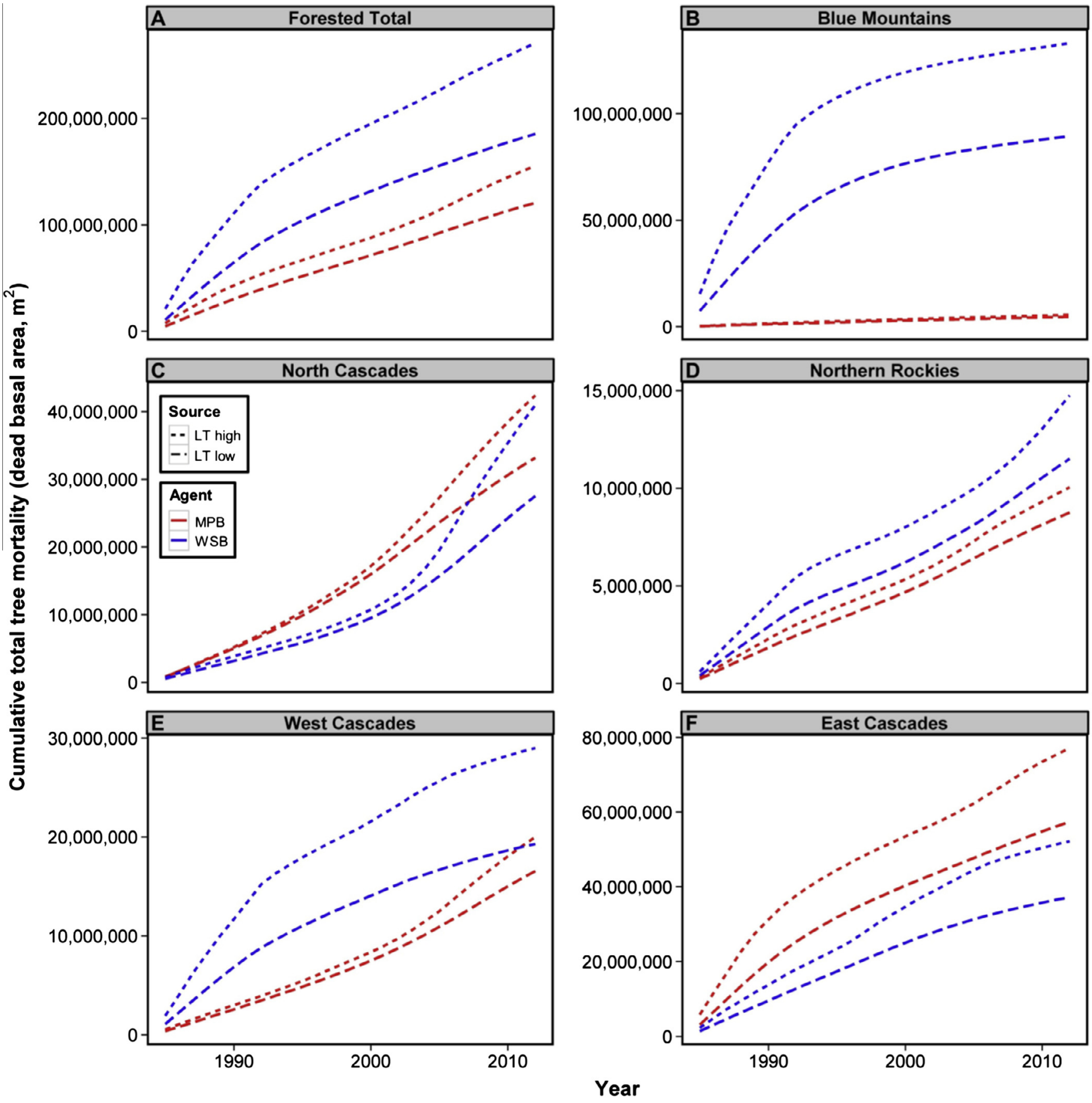

Fig. F1. Temporal patterns of cumulative mountain pine beetle (MPB; red) and western spruce budworm (WSB; blue) effects on tree mortality (dead tree basal area) from LandTrendr change detection (LT; 1984–2012) across forested ecoregions of the PNW. LT high refers to the high NBR slope threshold; LT low refers to the low NBR slope threshold (see Section 2). We calculate the "Forested Total" across all ecoregions but do not show the Coast Range and Klamath Mountains ecoregions here due to the absence of MPB and WSB activity. Note that the *Y* axes vary by ecoregion. Spatial patterns shown in Fig. 5. Annual effects shown in Fig. 6. (For interpretation of the references to color in this figure legend, the reader is referred to the web version of this article.)

References

Azuma, D.L., 2010. The effects of a western spruce budworm outbreak on the dead wood component in relation to ownership in forests of Eastern Oregon. West. J. Appl. For. 25, 176–180.

Bechtold, W.A., Patterson, P.L., 2005. The enhanced Forest Inventory and Analysis Program–national sampling design and estimation procedures. Gen Tech Rep SRS-GTR-80. USDA Forest Service, Southern Research Station, Asheville, NC.

Bentz, B.J., Regniere, J., Fettig, C.J., Hansen, E.M., Hayes, J.L., Hicke, J.A., Kelsey, R.G., Negron, J.F., Seybold, S.J., 2010. Climate change and bark beetles of the Western United States and Canada: direct and indirect effects. Bioscience 60, 602–613.

Ciesla, W.M., 2006. Aerial signatures of forest insect and disease damage in the western United States. Forest Health Technology Team, FHTET-01-06. USDA Forest Service, Ft. Collins CO.

Cohen, W.B., Goward, S.N., 2004. Landsat's role in ecological applications of remote sensing. Bioscience 54, 535–545.

Cohen, W.B., Maiersperger, T.K., Gower, S.T., Turner, D.P., 2003. An improved strategy for regression of biophysical variables and Landsat ETM+ data. Remote Sens. Environ. 84, 561–571.

Cohen, W.B., Yang, Z.G., Kennedy, R.E., 2010. Detecting trends in forest disturbance and recovery using yearly Landsat time series: 2. TimeSync – tools for calibration and validation. Remote Sens. Environ. 114, 2911–2924.

Crist, E.P., Cicone, R.C., 1984. A physically-based transformation of the thematic mapper data – the TM tassled cap. IEEE Trans. Geosci. Remote Sens. GE-22, 256–263.

Eidenshink, J., Schwind, B., Brewer, K., Zhu, Z.L., Quayle, B., Howard, S., 2007. A project for monitoring trends in burn severity. Fire Ecol. 3, 3–21.

Flower, A., Gavin, D.G., Heyerdahl, E.K., Parsons, R.A., Cohn, G.M., 2014. Drought-triggered western spruce budworm outbreaks in the interior Pacific Northwest: a multi-century dendrochronological record. For. Ecol. Manag. 324, 16–27.

Franklin, J.F., Dyrness, C.T., 1973. Natural vegetation of Oregon and Washington. Gen Tech Rep PNW-GTR-8. USDA Forest Service, Pacific Northwest Forest and Range Experiment Station, Portland, OR.

Goheen, E.M., Willhite, E.A., 2006. Field guide to common diseases and insect pests of Oregon and Washington conifers. R6-NR-FID-PR-01-06, USDA Forest Service Pacific Northwest Region, Portland, OR.

Goodwin, N.R., Magnussen, S., Coops, N.C., Wulder, M.A., 2010. Curve fitting of time-series Landsat imagery for characterizing a mountain pine beetle infestation. Int. J. Remote Sens. 31, 3263–3271.

Haugo, R., Zanger, C., DeMeo, T., Ringo, C., Shlisky, A., Blankenship, K., Simpson, M., Mellen-McLean, K., Kertis, J., Stern, M., 2015. A new approach to evaluate forest structure restorations needs across Oregon and Washington, USA. For. Ecol. Manage. 335, 37–50.

Hessburg, P.F., Smith, B.G., Salter, R.B., Ottmar, R.D., Alvarado, E., 2000. Recent changes (1930s–1990s) in spatial patterns of interior northwest forests, USA. For. Ecol. Manage. 136, 53–83.

Hicke, J.A., Johnson, M.C., Jane, L.H.D., Preisler, H.K., 2012. Effects of bark beetle-caused tree mortality on wildfire. For. Ecol. Manage. 271, 81–90.

Hicke, J.A., Meddens, A.J.H., Allen, C.D., Kolden, C.A., 2013. Carbon stocks of trees killed by bark beetles and wildfire in the western United States. Environ. Res. Lett. 8.

Hummel, S., Agee, J.K., 2003. Western spruce budworm defoliation effects on forest structure and potential fire behavior. Northwest Sci. 77, 159–169.

Kennedy, R.E., Yang, Z.G., Cohen, W.B., 2010. Detecting trends in forest disturbance and recovery using yearly Landsat time series: 1. LandTrendr – temporal segmentation algorithms. Remote Sens. Environ. 114, 2897–2910.

Kennedy, R.E., Andréfouët, S., Cohen, W.B., Gómez, C., Griffiths, P., Hais, M., Healey, S.P., Helmer, E.H., Hostert, P., Lyons, M.B., Meigs, G.W., Pflugmacher, D., Phinn, S.R., Powell, S.L., Scarth, P., Sen, S., Shroeder, T.A., Schneider, A., Sonnenschein, R., Vogelmann, J.E., Wulder, M.A., Zhu, Z., 2014. Bringing an ecological view of change to Landsat-based remote sensing. Front. Ecol. Environ. 12 (6), 339–346.

Key, C.H., Benson, N.C., 2006. Landscape assessment: ground measure of severity, the Composite Burn Index; and remote sensing of severity, the Normalized Burn Ratio. In: FIREMON: Fire Effects Monitoring and Inventory System, Gen Tech Rep RMRS-GTR-164-CD. USDA Forest Service, Rocky Mountain Research Station, Fort Collins CO.

Littell, J.S., McKenzie, D., Peterson, D.L., Westerling, A.L., 2009. Climate and wildfire area burned in western U.S. ecoprovinces, 1916–2003. Ecol. Appl. 19, 1003–1021.

Littell, J.S., Oneil, E.E., McKenzie, D., Hicke, J.A., Lutz, J.A., Norheim, R.A., Elsner, M.M., 2010. Forest ecosystems, disturbance, and climatic change in Washington State, USA. Clim. Change 102, 129–158.

Masek, J.G., Vermote, E.F., Saleous, N.E., Wolfe, R., Hall, F.G., Huemmrich, K.F., Gao, F., Kutler, J., Lim, T.K., 2006. A Landsat surface reflectance dataset for North America, 1990–2000. IEEE Geo. Remote Sens. Lett. 3 (1), 68–72.

Max, T.A., Schreuder, H.T., Hazard, J.W., Oswald, D.D., Teply, J., Alegria, J., 1996. The Pacific Northwest Region vegetation and inventory monitoring system. Res. Pap. PNW-RP-493. USDA Forest Service, Pacific Northwest Research Station, Portland, OR.

McKenzie, D., Gedalof, Z., Peterson, D.L., Mote, P., 2004. Climatic change, wildfire, and conservation. Conserv. Biol. 18, 890–902.

Meddens, A.J.H., Hicke, J.A., 2014. Spatial and temporal patterns of Landsat-based detection of tree mortality caused by a mountain pine beetle outbreak in Colorado, USA. For. Ecol. Manage. 322, 78–88.

Meddens, A.J.H., Hicke, J.A., Ferguson, C.A., 2012. Spatiotemporal patterns of observed bark beetle-caused tree mortality in British Columbia and the western United States. Ecol. Appl. 22, 1876–1891.

Meddens, A.J.H., Hicke, J.A., Vierling, L.A., Hudak, A.T., 2013. Evaluating methods to detect bark beetle-caused tree mortality using single-date and multi-date Landsat imagery. Remote Sens. Environ. 132, 49–58.

Meigs, G.W., Kennedy, R.E., Cohen, W.B., 2011. A Landsat time series approach to characterize bark beetle and defoliator impacts on tree mortality and surface fuels in conifer forests. Remote Sens. Environ. 115, 3707–3718.

Miller, J.D., Thode, A.E., 2007. Quantifying burn severity in a heterogeneous landscape with a relative version of the delta Normalized Burn Ratio (dNBR). Remote Sens. Environ. 109, 66–80.

Ohmann, J.L., Gregory, M.J., Spies, T.A., 2007. Influence of environment, disturbance, and ownership on forest vegetation of Coastal Oregon. Ecol. Appl. 17, 18–33.

Omernik, J.M., 1987. Ecoregions of the conterminous United States. Map (scale 1:7,500,000). Ann. Assoc. Am. Geogr. 77, 118–125.

Pflugmacher, D., Cohen, W.B., Kennedy, R.E., 2012. Using Landsat-derived disturbance history (1972–2010) to predict current forest structure. Remote Sens. Environ. 122, 146–165.

Preisler, H.K., Hicke, J.A., Ager, A.A., Hayes, J.L., 2012. Climate and weather influences on spatial temporal patterns of mountain pine beetle populations in Washington and Oregon. Ecology 93, 2421–2434.

Raffa, K.F., Aukema, B.H., Bentz, B.J., Carroll, A.L., Hicke, J.A., Turner, M.G., Romme, W.H., 2008. Cross-scale drivers of natural disturbances prone to anthropogenic amplification: the dynamics of bark beetle eruptions. Bioscience 58, 501–517.

Sanders, C.J., Stark, R.W., Mullins, E.J., Murphy, J. (Eds.), 1985. Recent advances in spruce budworms research. In: Proceedings of the CANUSA Spruce Budworms Research Symposium, Bangor, Maine, 16–20 September 1984. Canadian Forestry Service, Ottawa, Ontario, Canada.

Simard, M., Romme, W.H., Griffin, J.M., Turner, M.G., 2011. Do mountain pine beetle outbreaks change the probability of active crown fire in lodgepole pine forests? Ecol. Monogr. 81, 3–24.

Swetnam, T.W., Betancourt, J.L., 1998. Mesoscale disturbance and ecological response to decadal climatic variability in the American Southwest. J. Clim. 11, 3128–3147.

Swetnam, T.W., Lynch, A.M., 1993. Multicentury, regional-scale patterns of western spruce budworm outbreaks. Ecol. Monogr. 63, 399–424.

Vogelmann, J.E., Tolk, B., Zhu, Z.L., 2009. Monitoring forest changes in the southwestern United States using multitemporal Landsat data. Remote Sens. Environ. 113, 1739–1748.

Waring, R.H., Savage, T., Cromack Jr., K., Rose, C., 1992. Thinning and nitrogen fertilization in a grand fir stand infested with western spruce budworm. Part IV: an ecosystem management perspective. For. Sci. 38, 275–286.

Williams, D.W., Birdsey, R.A., 2003. Historical patterns of spruce budworm defoliation and bark beetle outbreaks in North American conifer forests: an atlas and description of digital maps. Gen Tech Rep NE-GTR-308. USDA Forest Service, Northeast Research Station, Newtown Square, PA.

Wulder, M.A., Dymond, C.C., White, J.C., Leckie, D.G., Carroll, A.L., 2006. Surveying mountain pine beetle damage of forests: a review of remote sensing opportunities. For. Ecol. Manage. 221, 27–41.

Zald, H.S.J., Ohmann, J.L., Roberts, H.M., Gregory, M.J., Henderson, E.B., McGaughey, R.J., Braaten, J., 2014. Influence of lidar, Landsat imagery, disturbance history, plot location accuracy, and plot size on accuracy of imputation maps of forest composition and structure. Remote Sens. Environ. 143, 26–38.

Zhu, Z., Woodcock, C.E., 2012. Object-based cloud and cloud shadow detection in Landsat imagery. Remote Sens. Environ. 118, 83–94.